Journal of Naval Architecture and Marine Engineering
June, 2011
DOI: 10.3329/jname.v8i1.6054 http://www.banglajol.info

SORET AND DUFOUR EFFECTS ON TRANSIENT MHD FLOW PAST A SEMI-INFINITE VERTICAL POROUS PLATE WITH CHEMICAL REACTION

S. Shivaiah[1] and J. Anand Rao[2]

[1] Department of Mathematics, BVRIT, Narsapur, Medak-502313, (A.P), India.
[2]Department of Mathematics, Osmania University, Hyderabad-500007,(A.P), India.
Email: sreddy7@yahoo.co.in

Abstract:

In the present steady, an unsteady two-dimensional MHD flow chemical reacting fluid past a semi-infinite vertical porous plate with Soret and Dufour effects are analyzed. The dimensionless governing equations are solved numerically by a finite element method. Computations are performed for a wide range of the governing flow parameters, viz., the thermal Grashof number, solutal Grashof number, Magnetic field parameter, Permeability parameter, Prandtl number, Heat absorption parameter, Dufour number, Schmidt number, Chemical reaction parameter and Soret number. The effects of these flow parameters on the velocity, temperature and concentration are shown graphically. Finally, the effects of various parameters on the skin-friction coefficient, Nusselt number and Sherwood number are shown in Tables.

Keywords: MHD, Soret and Dufour effects, Porous plate, Chemical reaction.

NOMENCLATURE:

T'	temperature of the fluid in near the plate	C'	species concentration in the fluid
p'	the pressure	g	acceleration due to gravity
t'	time	t	dimensionless time
c_p	specific heat at constant pressure	c_s	concentration susceptibility
D_m	mass diffusion coefficient	k_T	thermal diffusion ratio
k	thermal conductively	T_m	mean fluid temperature
K'	permeability of the porous medium	B_0	applied magnetic field
Gr	thermal Grashof number	Gm	solutal Grashof number
M	magnetic parameter	K	Permeability parameter
Q	heat source parameter	Pr	Prandtl number
Sc	Schmidt number	Du	Dufour number
K_r	chemical reaction parameter	Sr	Soret number
θ	dimensionless temperature	C	dimensionless concentration
u'	velocity of the fluid	u	dimensionless velocity
u', v'	velocity components in	U_0	mean velocity
x', y'	direction respectively		

Greek Symbols

α	the fluid thermal diffusivity	ρ	density of the fluid
β	coefficient of volume expansion due to concentration	c_p	specific heat at constant pressure
β^*	coefficient of volume expansion due to concentration	σ	electrical conductivity

 Received on: September 2010

		Subscripts	
μ	viscosity of the fluid	w	condition at the wall
ν	kinematic viscosity	∞	free stream conditions

1. Introduction

Combined heat and mass transfer (or double-diffusion) in fluid-saturated porous media finds applications in a variety of engineering processes such as heat exchanger devices, petroleum reservoirs, chemical catalytic reactors and processes, geothermal and geophysical engineering, moisture migration in a fibrous insulation and nuclear waste disposal and others. Double diffusive flow is driven by buoyancy due to temperature and concentration gradients. Combined buoyancy-generated heat and mass transfer, due to temperature and concentration variations, in fluid-saturated porous media, have several important applications in a variety of engineering process including heat exchanger devices, petroleum reservoirs, chemical catalytic reactors, solar energy porous wafer collector systems, ceramic materials, migration of moisture through air contained in fibrous insulations and grain storage installations, and the dispersion of chemical contaminants through water-saturated soil, superconvecting geothermics etc. The vertical free convection boundary layer flow in porous media owing to combined heat and mass transfer has been investigated.

There has been renewed interest in studying magneto hydrodynamic (MHD) flow and heat transfer in porous and non-porous media due to the effect of magnetic field on the boundary layer flow control and on the performance of many systems using electrically conducting fluids. In addition, this type of flow finds applications in many engineering problems such as MHD generators, plasma studies, nuclear reactors, and geothermal energy extractions. Soundalgekar (1973) obtained approximate solutions for the two-dimensional flow of an incompressible, viscous fluid past an infinite vertical porous plate with constant suction normal to the plate. Lai and Kulacki (1991) used the series expansion method to investigate coupled heat and mass transfer by natural convection from vertical surface in a porous medium. Kim (2000) presented an analysis of an unsteady MHD convection flow past a vertical moving plate embedded in a porous medium in the presence of transverse magnetic field. Helmy (1998) studied MHD unsteady free convection flow past a vertical porous plate. Soundalgekar (1977) studied the free convection flow past an impulsively started infinite vertical plate, when it is cooled or heated by free convection currents. Kafoussias et al. (1979) studied the effects of suction on the flow field, in the problem. Nanousis et al. (1980) extended this problem to magnetohydrodynamics.

In all these studies Soret / Dufour effects are assumed to be negligible. Such effects are significant when density differences exist in the flow regime. For example when species are introduced at a surface in fluid domain, with different (lower) density than the surrounding fluid, both Soret and Dufour effects can be significant. Also, when heat and mass transfer occur simultaneously in a moving fluid, the relations between the fluxes and the driving potentials are of more intricate nature. It has been found that an energy flux can be generated not only by temperature gradients but by composition gradients as well. The energy flux caused by a composition gradient is called the Dufour or diffusion-thermo effect. On the other hand, mass fluxes can also be created by temperature gradients and this is called the Soret or thermal-diffusion effect. The thermal-diffusion (Soret) effect, for instance, has been utilized for isotope separation, and in mixture between gases with very light molecular weight (H2, He) and of medium molecular weight (N2, air), the diffusion-thermo (Dufour) effect was found to be of a considerable magnitude such that it cannot be ignored (Eckert and Drake 1972). In view of the importance of this diffusion-thermo effect, Jha and Singh (1990) studied the free-convection and mass transfer flow about an infinite vertical flat plate moving impulsively in its own plane, taking into account the Soret effects. Kafoussias (1992) studied the same problem in the case of MHD flow. Kafoussias and Williams (Kafoussias and Williams 1995) presented the same effects on mixed free-forced convective and mass transfer boundary layer flow with temperature dependent viscosity.

Chamkha and Takhar (2001) are used the blottner difference method to study laminar free convection flow of air past a semi infinite vertical plate in the presence of chemical species concentration and thermal radiation effects. Ibrahim (2008) studied the effects of chemical reaction and radiation absorption on transient hydro magnetic natural convection flow with wall transpiration and heat source.

However, the interaction of Soret and Dufour effects on transient MHD flow in a porous plate with chemical reaction has received a little attention. Hence, the object of the present chapter is to analyze the Soret and Dufour effects on transient MHD flow past a semi-infinite vertical porous plate by taking chemical reaction into account. The governing equations are transformed by using similarity transformation and the resultant

dimensionless equations are solved numerically using the finite element method. The effects of various governing parameters on the velocity, temperature, concentration, skin-friction coefficient, Nusselt number and Sherwood number are shown in figures and tables and analyzed in detail.

2. Mathematical Formulation of the Problem

An unsteady two-dimensional hydromagnetic flow of a viscous incompressible, electrically conducting and chemical reacting fluid past a semi-infinite permeable vertical moving plate in a porous medium is considered. The flow is assumed to be in the x' - direction, which is taken along the semi-infinite plate and y' - axis normal to it. The physical model and coordinate system of the problem is shown in Fig. A. A uniform magnetic field is applied in the direction perpendicular to the plate. The fluid is assumed to be slightly conducting, and hence the magnetic Reynolds number is much less than unity and the induced magnetic field is negligible in comparison with the applied magnetic field. It is further assumed that there is no applied voltage, so that electric field is absent. It is also assumed that all the fluid properties are constant except that of the influence of the density variation with temperature and concentration in the body force term (Boussinesq's approximation).

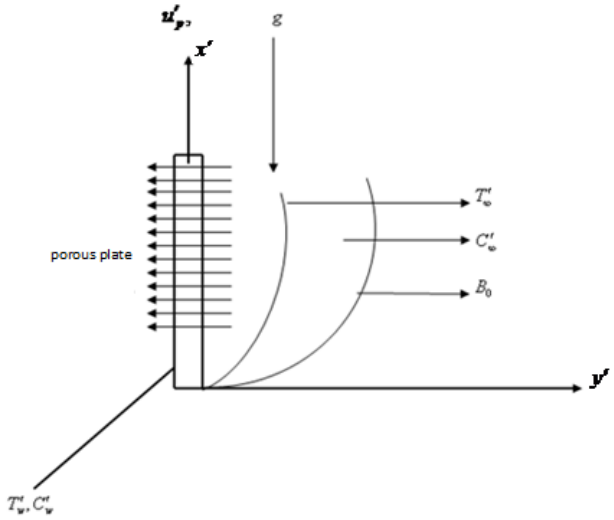

Fig. A. Physical model and coordinate system of the problem

Based on above assumptions, the governing equations can be written as:

Continuity equation:

$$\frac{\partial v'}{\partial y'} = 0 \tag{1}$$

Momentum equation:

$$\frac{\partial u'}{\partial t'} + v'\frac{\partial u'}{\partial y'} = -\frac{1}{\rho}\frac{\partial p'}{\partial x'} + \nu\frac{\partial^2 u'}{\partial y'^2} + g\beta\left(T' - T'_\infty\right) + g\beta^*\left(C' - C'_\infty\right) - \nu\frac{u'}{K'} - \frac{\sigma B_0^2 u'}{\rho} \tag{2}$$

Energy equation:

$$\frac{\partial T'}{\partial t'} + v'\frac{\partial T'}{\partial y} = \alpha\frac{\partial^2 T'}{\partial y'^2} - \frac{Q_0}{\rho c_p}\left(T' - T'_\infty\right) + \frac{D_m k_T}{c_s c_p}\frac{\partial^2 C'}{\partial y'^2} \tag{3}$$

Species equation:

$$\frac{\partial C'}{\partial t'} + v'\frac{\partial C'}{\partial y'} = D_m\frac{\partial^2 C'}{\partial y'^2} - k'_r C' + \frac{D_m k_T}{T_m}\frac{\partial^2 T'}{\partial y'^2} \tag{4}$$

The boundary conditions for the velocity, temperature and concentration fields are:

$$\begin{aligned} &u' = u'_p, \quad T' = T'_\infty + \varepsilon\left(T'_w - T'_\infty\right)e^{n't'}, \quad C' = C'_\infty + \varepsilon\left(C'_w - C'_\infty\right)e^{n't'} && at \;\; y' = 0 \\ &u' = U'_\infty = U_0\left(1 + \varepsilon e^{n't'}\right), \quad T' \to T'_\infty, \quad C' \to C'_\infty && as \;\; y' \to \infty \end{aligned} \tag{5}$$

Where u'_p is the plate velocity, T'_w and C'_w are the wall dimensional temperature and concentration respectively, T'_∞ and C'_∞ are the free stream dimensional temperature and concentration respectively, U'_∞ the free stream velocity, U_0 and n' -the constant.

From the equation (1), it is clear that suction velocity normal to the plate is either a constant or function of time. Hence, it is assumed in the form

$$v' = -V_0\left(1 + \varepsilon\, A e^{n't'}\right) \tag{6}$$

Where A is a real positive constant, ε and εA are small values less than unity and V_0 is scale of suction velocity which is non zero positive constant. Outside boundary layer, equation (2) gives

$$-\frac{1}{\rho}\frac{\partial p'}{\partial x'} = \frac{dU'_\infty}{dt'} + \frac{\nu U'_\infty}{K'} + \frac{\sigma B'_0 U'_\infty}{\rho} \tag{7}$$

In order to write the governing equations and the boundary conditions in dimensionless form, the following non-dimensional quantities are introduced.

$$\begin{aligned} &u = \frac{u'}{U_0},\ v = \frac{v'}{V_0},\ Y = \frac{V_0 y'}{\nu},\ u_p = \frac{u'_p}{U_0},\ U_\infty = \frac{U'_\infty}{U_0},\ n = \frac{n'\nu}{V_0^2},\ t = \frac{t'V_0^2}{\nu},\ \theta = \frac{T' - T'_\infty}{T'_w - T'_\infty},\ C = \frac{C' - C'_\infty}{C'_w - C'_\infty}, \\ &K = \frac{K'V_0^2}{\nu^2},\ Pr = \frac{\nu\rho C_p}{k} = \frac{\nu}{\alpha},\ Sc = \frac{\nu}{D},\ M = \frac{\sigma B_0^2 \nu}{\rho V_0^2},\ Q = \frac{Q_0 \nu}{\rho c_p V_0^2},\ Du = \frac{D_m k_T\left(C'_w - C'_\infty\right)}{c_s c_p\left(T'_w - T'_\infty\right)}, \\ &Gr = \frac{\nu\beta g(T'_w - T'_\infty)}{U_0 V_0^2},\ Gm = \frac{\nu\beta^* g(C'_w - C'_\infty)}{U_0 V_0^2},\quad K_r = \frac{k'_r \nu}{V_0^2},\ Sr = \frac{D_m k_T\left(T'_w - T'_\infty\right)}{\nu T_m\left(C'_w - C'_\infty\right)} \end{aligned} \tag{8}$$

In view of Equations (5), (6), (7) and (8), Equations (2), (3) and (4) reduce to the following dimensionless form.

$$\frac{\partial u}{\partial t} - (1 + \varepsilon A e^{nt})\frac{\partial u}{\partial Y} = \frac{dU_\infty}{dt} + \frac{\partial^2 u}{\partial Y^2} + Gr\theta + GmC + M_1(U_\infty - u) \tag{9}$$

$$\frac{\partial \theta}{\partial t} - (1 + \varepsilon A e^{nt})\frac{\partial \theta}{\partial Y} = \frac{1}{\Pr}\frac{\partial^2 \theta}{\partial Y^2} - Q\theta + Du\frac{\partial^2 C}{\partial Y^2} \tag{10}$$

$$\frac{\partial C}{\partial t} - (1 + \varepsilon A e^{nt})\frac{\partial C}{\partial Y} = \frac{1}{Sc}\frac{\partial^2 C}{\partial Y^2} - K_r C + Sr\frac{\partial^2 \theta}{\partial Y^2} \tag{11}$$

Where $M_1 = \left(M + \frac{1}{K}\right)$

The corresponding boundary conditions are:

$$\begin{aligned} &u = u_p,\ \theta = 1 + \varepsilon e^{nt},\ C = 1 + \varepsilon e^{nt} && at\ Y = 0 \\ &u \to U_\infty = 1 + \varepsilon e^{nt},\ \theta \to 0,\ C \to 0 && as\ Y \to \infty \end{aligned} \tag{12}$$

3. Method of solution

The Galerkin expansion for the differential equation (9) becomes

$$\int_{y_j}^{y_k} N^{(e)^T}\left[\frac{\partial^2 u^{(e)}}{\partial y^2}+P\frac{\partial u^{(e)}}{\partial y}-\frac{\partial u^{(e)}}{\partial t}-M_1 u^{(e)}+R\right]dy=0 \tag{13}$$

Where

$$P=1+A\varepsilon e^{nt},\quad R=n\varepsilon e^{nt}+Gr\theta+GmC+M_1U_\infty$$

Let the linear piecewise approximation solution

$$u^{(e)}=N_j(y)u_j(t)+N_k(y)u_k(t)=N_j u_j+N_k u_k$$

Where $N_j=\dfrac{y_k-y}{y_k-y_j}$, $N_k=\dfrac{y-y_j}{y_k-y_j}$

$$N^{(e)^T}=\begin{bmatrix}N_j & N_k\end{bmatrix}^T=\begin{bmatrix}N_j\\ N_k\end{bmatrix}$$

$$N^{(e)^T}\frac{\partial u^{(e)}}{\partial y}\Bigg\}_{y_j}^{y_k}-\int_{y_j}^{y_k}\left\{\frac{\partial N^{(e)^T}}{\partial y}\frac{\partial u^{(e)}}{\partial y}-N^{(e)^T}\left(P\frac{\partial u^{(e)}}{\partial y}+\frac{\partial u^{(e)}}{\partial t}+M_1u^{(e)}-R\right)\right\}dy=0 \tag{14}$$

Neglecting the first term in equation (14) we gets

$$\int_{y_j}^{y_k}\left\{\frac{\partial N^{(e)^T}}{\partial y}\frac{\partial u^{(e)}}{\partial y}-N^{(e)^T}\left(P\frac{\partial u^{(e)}}{\partial y}-\frac{\partial u^{(e)}}{\partial t}-M_1u^{(e)}+R\right)\right\}dy=0$$

$$\frac{1}{l^{(e)}}\begin{bmatrix}1 & -1\\ -1 & 1\end{bmatrix}\begin{bmatrix}u_j\\ u_k\end{bmatrix}-\frac{P}{2}\begin{bmatrix}-1 & 1\\ -1 & 1\end{bmatrix}\begin{bmatrix}u_j\\ u_k\end{bmatrix}+\frac{l^{(e)}}{6}\begin{bmatrix}2 & 1\\ 1 & 2\end{bmatrix}\begin{bmatrix}\dot{u}_j\\ \dot{u}_k\end{bmatrix}+\frac{M_1l^{(e)}}{6}\begin{bmatrix}2 & 1\\ 1 & 2\end{bmatrix}\begin{bmatrix}u_j\\ u_k\end{bmatrix}=R\frac{l^{(e)}}{2}\begin{bmatrix}1\\ 1\end{bmatrix}$$

Where $l^{(e)}=y_k-y_j=h$ and dot denotes the differentiation with respect to t.

We write the element equations for the elements $y_{i-1}\le y\le y_i$ and $y_i\le y\le y_{i+1_i}$ assemble three element equations, we obtain

$$\frac{1}{l^{(e)^2}}\begin{bmatrix}1 & -1 & 0\\ -1 & 2 & -1\\ 0 & -1 & 1\end{bmatrix}\begin{bmatrix}u_{i-1}\\ u_i\\ u_{i+1}\end{bmatrix}-\frac{P}{2l^{(e)}}\begin{bmatrix}-1 & 1 & 0\\ -1 & 0 & 1\\ 0 & -1 & 1\end{bmatrix}\begin{bmatrix}u_{i-1}\\ u_i\\ u_{i+1}\end{bmatrix}+\frac{1}{6}\begin{bmatrix}2 & 1 & 0\\ 1 & 4 & 1\\ 0 & 1 & 2\end{bmatrix}\begin{bmatrix}\dot{u}_{i-1}\\ \dot{u}_i\\ \dot{u}_{i+1}\end{bmatrix}+\frac{M_1}{6}\begin{bmatrix}2 & 1 & 0\\ 1 & 4 & 1\\ 0 & 1 & 2\end{bmatrix}\begin{bmatrix}u_{i-1}\\ u_i\\ u_{i+1}\end{bmatrix}=\frac{R}{2}\begin{bmatrix}1\\ 2\\ 1\end{bmatrix} \tag{15}$$

Now put row corresponding to the node i to zero, from Equation (15) the difference schemes is

$$\frac{1}{l^{(e)^2}}\left[-u_{i-1}+2u_i-u_{i+1}\right]-\frac{P}{2l^{(e)}}\left[-u_{i-1}+u_{i+1}\right]+\frac{1}{6}\left[\dot{u}_{i-1}+4\dot{u}_i+\dot{u}_{i+1}\right]+\frac{M_1}{6}\left[u_{i-1}+4u_i+u_{i+1}\right]=R$$

Applying Crank-Nicholson method to the above equation then we gets

$$A_1u_{i-1}^{j+1}+A_2u_i^{j+1}+A_3u_{i+1}^{j+1}=A_4u_{i-1}^{j}+A_5u_i^{j}+A_6u_{i+1}^{j}+R^* \tag{16}$$

Where

$A_1=2-6r+3Phr+M_1k$, $A_2=8+12r+4M_1k$,

$A_3=2-6r-3Phr+M_1k$, $A_4=2+6r-3Phr-M_1k$,

$A_5=8-12r-4M_1k$, $A_6=2+6r+3Phr-M_1k$

$R^*=12(Gr)k\theta_i^j+12(Gm)k\phi_i^j+12kM_1U_\infty+12kn\text{æ}e^{nt}$;

Applying similar procedure to equation (12) and (13) then we gets

$$B_1\theta_{i-1}^{j+1}+B_2\theta_i^{j+1}+B_3\theta_{i+1}^{j+1}=B_4\theta_{i-1}^{j}+B_5\theta_i^{j}+B_6\theta_{i+1}^{j}+R^{**} \tag{17}$$

$$C_1C_{i-1}^{j+1}+C_2C_i^{j+1}+C_3C_{i+1}^{j+1}=C_4C_{i-1}^{j}+C_5C_i^{j}+C_6C_{i+1}^{j}+R^{***} \tag{18}$$

Where

$B_1=2\,\mathrm{Pr}-6r+3\,\mathrm{Pr}\,Phr+\mathrm{Pr}\,Qk$, $B_2=8\,\mathrm{Pr}+12r+4\,\mathrm{Pr}\,Qk$,

$B_3=2\,\mathrm{Pr}-6r-3\,\mathrm{Pr}\,Phr+\mathrm{Pr}\,Qk$, $B_4=2\,\mathrm{Pr}+6r-3\,\mathrm{Pr}\,Phr-\mathrm{Pr}\,Qk$,

$B_5=8\,\mathrm{Pr}-12r-4\,\mathrm{Pr}\,Qk$, $B_6=2\,\mathrm{Pr}+6r+3\,\mathrm{Pr}\,Phr-\mathrm{Pr}\,Qk$

$R^{**}=12r\,\mathrm{Pr}\,Du(C[i-1]-2C[i]+C[i+1])$

$C_1=2Sc-6r+3PScrh+ScK_rk$, $C_2=8Sc+12r+4ScK_rk$,

$C_3=2Sc-6r-3PScrh+ScK_rk$, $C_4=2Sc+6r-3PScrh-ScK_rk$,

$C_5=8Sc-12r-4ScK_rk$, $C_6=2Sc+6r+3PScrh-ScK_rk$

$R^{***}=12rScSr\,(\theta[i-1]-2\theta[i]+\theta[i+1])$

Here $r=\frac{k}{h^2}$ and h,k are the mesh sizes along $y-$direction and time $t-$direction respectively. Index i refers to the space and j refers to the time. In Equations (16)-(18), taking $i=1(1)n$ and using initial and boundary conditions (12), the following system of equations are obtained:

$$A_i X_i = B_i \qquad \text{i=1(1)3} \tag{19}$$

Where A_i's are matrices of order n and X_i, B_i's column matrices having $n-$components. The solutions of above system of equations are obtained by using Thomas algorithm for velocity, temperature and concentration. Also, numerical solutions for these equations are obtained by C-program. In order to prove the convergence and stability of finite element method, the same C-program was run with slightly changed values of h and k and no significant change was observed in the values of u, θ and C. Hence, the finite element method is stable and convergent.

The skin-friction, Nusselt number and Sherwood number are important physical parameters for this type of boundary layer flow.

The skin-friction at the plate, which in the non-dimensional form is given by

$$C_f = \frac{\tau'_w}{\rho U_0 V_0} = \left(\frac{\partial u}{\partial Y}\right)_{Y=0} \tag{20}$$

The rate of heat transfer coefficient, which in the non-dimensional form in terms of the Nusselt number is given by

$$Nu = -x\frac{\left(\frac{\partial T'}{\partial y'}\right)_{y'=0}}{T'_w - T'_\infty} \Rightarrow Nu\,\mathrm{Re}_x^{-1} = -\left(\frac{\partial \theta}{\partial Y}\right)_{Y=0} \tag{21}$$

The rate of mass transfer coefficient, which in the non-dimensional form in terms of the Sherwood number, is given by

$$Sh = -x\frac{\left(\frac{\partial C'}{\partial y'}\right)_{y'=0}}{C'_w - C'_\infty} \Rightarrow Sh\,\mathrm{Re}_x^{-1} = -\left(\frac{\partial C}{\partial Y}\right)_{Y=0} \tag{22}$$

Where $\mathrm{Re}_x = \frac{V_0 x}{\nu}$ is the local Reynolds number.

4. Results and Discussion

As a result of the numerical calculations, the dimensionless velocity, temperature and concentration distributions for the flow under consideration are obtained and their behaviour have been discussed for variations in the governing parameters viz., the thermal Grashof number Gr, solutal Grashof number Gm, magnetic field parameter M, permeability parameter K, Prandtl number Pr, heat absorption parameter Q, Dufour number Du, Schmidt number Sc, Soret number *Sr* and chemical reaction parameter K_r. Here we fixed $\varepsilon = 0.1$, $n = 0.1$, $t = 1.0$, $A = 0.5$.

The influence of the thermal Grashof number on the velocity is presented in Fig 1. The thermal Grashof number signifies the relative effect of the thermal buoyancy force to the viscous hydrodynamic force in the boundary layer. As expected, it is observed that there is a rise in the velocity due to the enhancement of thermal buoyancy force. Here, the positive values of Gr correspond to cooling of the plate. Also, as Gr increases, the peak values of the velocity increases rapidly near the porous plate and then decays smoothly to the free stream velocity.

Fig 2 presents typical velocity profiles in the boundary layer for various values of the solutal Grashof number Gm, while all other parameters are kept at some fixed values. The solutal Grashof number Gm defines the ratio of the species buoyancy force to the viscous hydrodynamic force. As expected, the fluid velocity increases

and the peak value is more distinctive due to increase in the species buoyancy force. The velocity distribution attains a distinctive maximum value in the vicinity of the plate and then decreases properly to approach the free stream value.

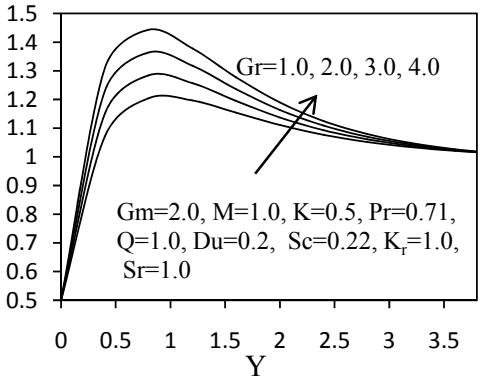

Fig. 1: Velocity profiles for different values of Gr

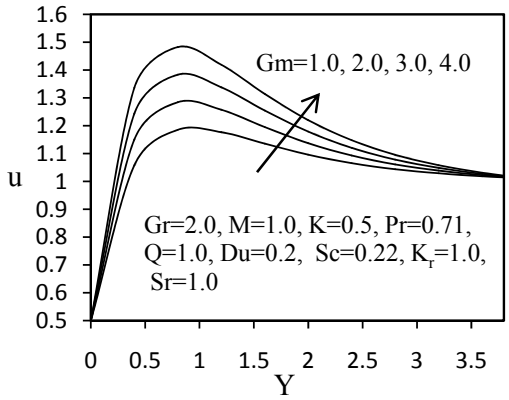

Fig. 2: Velocity profiles for different values of Gm

For various values of the magnetic parameter M , the velocity profiles are plotted in Fig 3. It can be seen that as M increases, the velocity decreases. This result qualitatively agrees with the expectations, since the magnetic field exerts a retarding force on the flow.

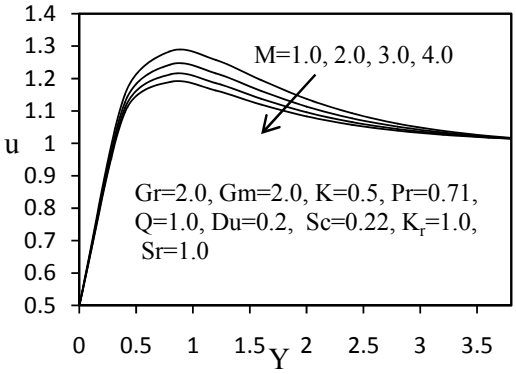

Fig. 3: Velocity profiles for different values of M

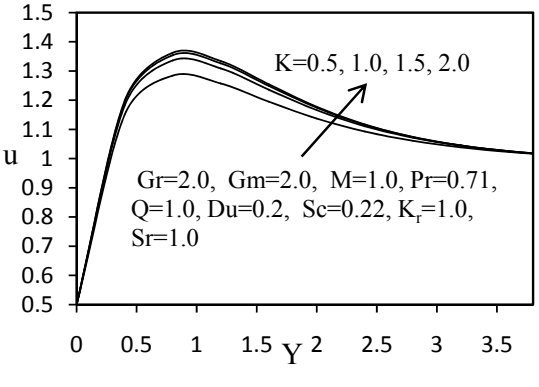

Fig. 4: Velocity profiles for different values of K

The effect of the permeability parameter K on the velocity field is shown in Fig 4. An increase the resistance of the porous medium which will tend to decelerate the flow and reduce the velocity. This behavior is evident from Fig 4.

Figs 5(a) and 5(b) illustrate the velocity and temperature profiles for different values of the Prandtl number Pr . The Prandtl number defines the ratio of momentum diffusivity to thermal diffusivity. The numerical results show that the effect of increasing values of Prandtl number results in a decreasing velocity (Fig 5 (a)). From Fig 5 (b), it is observed that an increase in the Prandtl number results a decrease of the thermal boundary layer thickness and in general lower average temperature within the boundary layer. The reason is that smaller values of Pr are equivalent to increasing the thermal conductivities, and therefore heat is able to diffuse away from the heated plate more rapidly than for higher values of Pr . Hence in the case of smaller Prandtl numbers as the boundary layer is thicker and the rate of heat transfer is reduced.

Figs 6(a) and 6(b) illustrate the velocity and temperature profiles for different values of heat absorption parameter Q , the numerical results show that the effect of increasing values of heat absorption parameter result in a decreasing velocity and temperature.

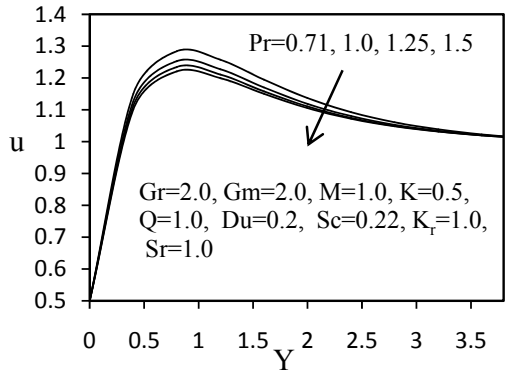

Fig.5(a): Velocity profiles for different values of Pr

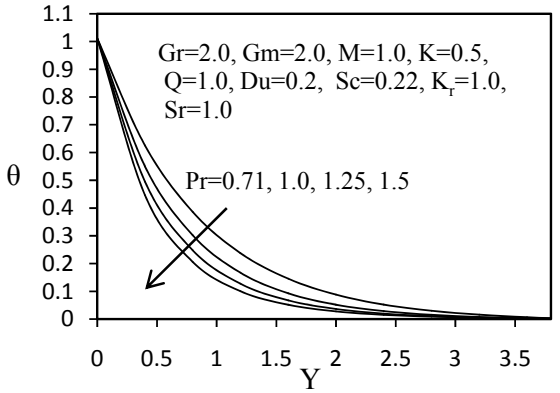

Fig.5(b) 2: Temperature profiles for different values of Pr

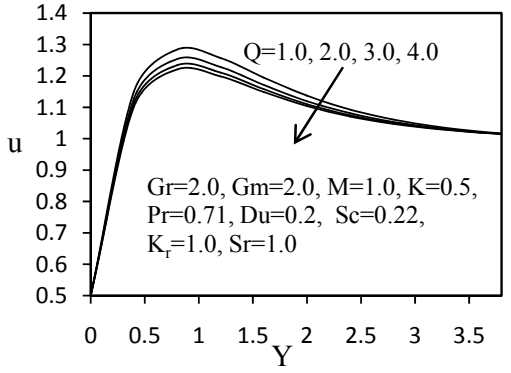

Fig. 6(a): Velocity profiles for different values of Q

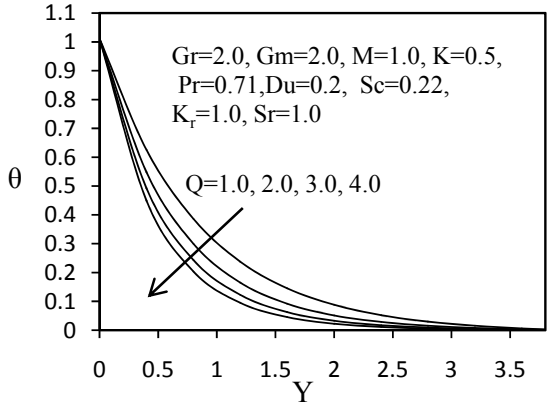

Fig.6(b): Temperature profiles for different values of Q

For different values of the Dufour number Du, the velocity and temperature profiles are plotted in Figs 7(a) and 7(b) respectively. The Dufour number Du signifies the contribution of the concentration gradients to the thermal energy flux in the flow. It is found that an increase in the Dufour number causes a rise in the velocity and temperature throughout the boundary layer. For, the temperature profiles decay smoothly from the plate to the free stream value. However for, a distinct velocity overshoot exists near the plate, and thereafter the profile falls to zero at the edge of the boundary layer.

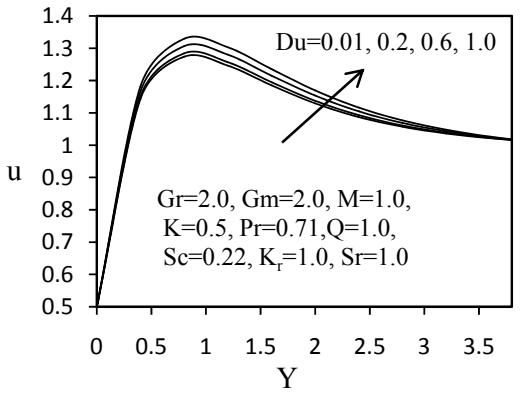

Fig.7(a): Velocity profiles for different values of Du

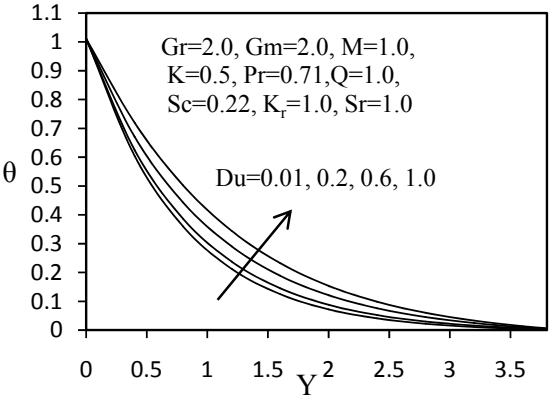

Fig.7(b): Temperature profiles for different values of Du

The influence of the Schmidt number Sc on the velocity and concentration profiles are plotted in Figs 8(a) and 8(b) respectively. The Schmidt number embodies the ratio of the momentum to the mass diffusivity. The Schmidt number therefore quantifies the relative effectiveness of momentum and mass transport by diffusion in

the hydrodynamic (velocity) and concentration (species) boundary layers. As the Schmidt number increases the concentration decreases. This causes the concentration buoyancy effects to decrease yielding a reduction in the fluid velocity. The reductions in the velocity and concentration profiles are accompanied by simultaneous reductions in the velocity and concentration boundary layers. These behaviors are clear from Figs 8(a) and 8(b).

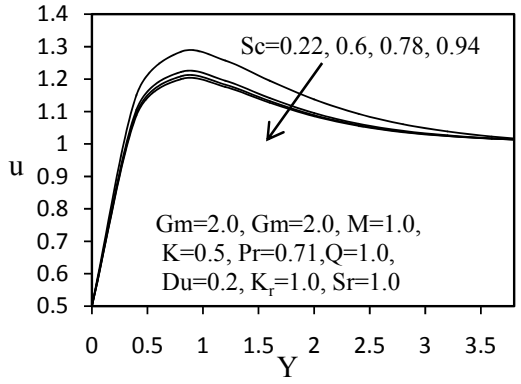

Fig.8(a): Velocity profiles for different values of Sc

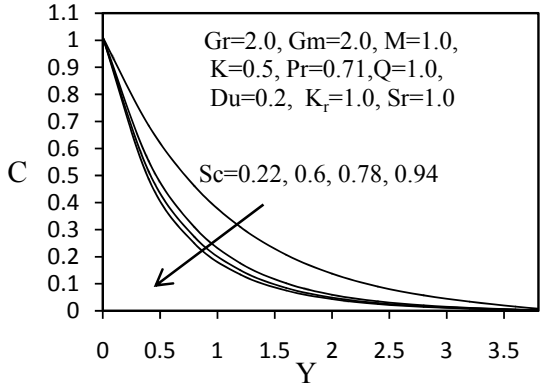

Fig.8(b): Concentration profiles for different values of Sc

Figs 9(a) and 9(b) depict the velocity and concentration profiles for different values of the Soret number Sr. The Soret number Sr defines the effect of the temperature gradients inducing significant mass diffusion effects. It is noticed that an increase in the Soret number Sr results in an increase in the velocity and concentration within the boundary layer.

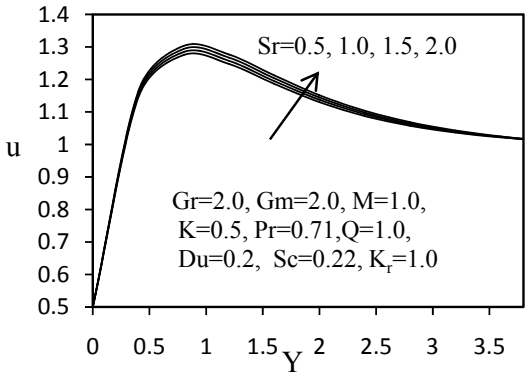

Fig.9(a): Velocity profiles for different values of Sr

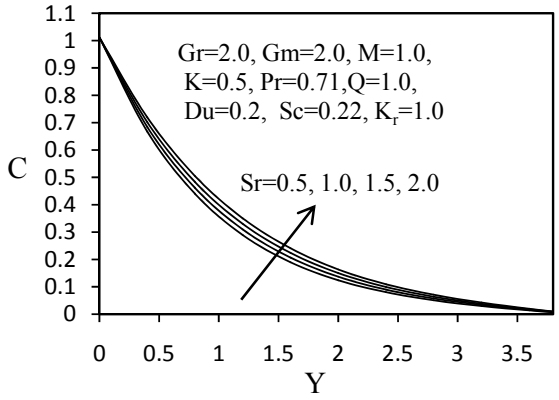

Fig.9(b): Concentration profiles for different values of Sr

Figs 10(a) and 10(b) illustrates the behavior velocity and concentration for different values of chemical reaction parameter K_r. It is observed that an increase in leads to a decrease in both the values of velocity and concentration. A distinct velocity escalation occurs near the wall after which profiles decay smoothly to the stationary value in free stream. Chemical reaction therefore boosts momentum transfer i.e. accelerates the flow.

The effects of various governing parameters on the skin-friction coefficient, Nusselt number and the Sherwood number are shown in Tables 1 to 3. From Table 1, it is observed that as Gr or Gm or K increases, the skin-friction coefficient increases, where as the skin-friction coefficient decreases as M increases. From Table 2, it is noticed that as $\Pr$ or Q increases, the skin-friction coefficient decreases while the Nusselt number increases and Du increases, the skin-friction coefficient increases while the Nusselt number decreases. From Table 3, it is found that as Sc or K_r increases, the skin-friction coefficient decreases while the Sherwood number increases and Sr increases, the skin-friction coefficient increases while the Sherwood number decreases.

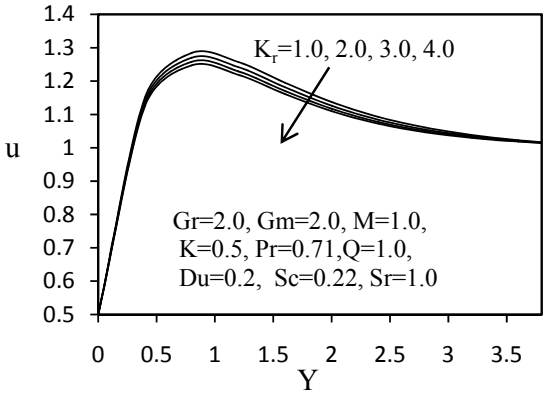

Fig.10(a) 1: Velocity profiles for different values of K_r

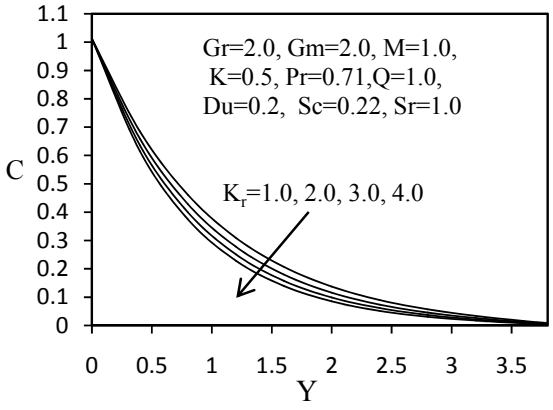

Fig.10(b): Concentration profiles for different values of K_r

Table 1 : Effect of Gr , Gm , M and K on C_f

($\Pr$ =0.71, Q =1.0, Du =0.2, Sc =0.22, Sr =1.0, K_r =1.0)

Gr	Gm	M	K	C_f
2.0	2.0	1.0	0.5	2.4723
4.0	2.0	1.0	0.5	3.1437
2.0	4.0	1.0	0.5	3.2259
2.0	2.0	2.0	0.5	2.4326
2.0	2.0	1.0	1.0	2.5333

Table 2 : Effect of $\Pr$, Q and Du on C_f and Nu

(Gr =2.0, Gm =2.0, M =1.0, K =0.5, Sc =0.22, K_r =1.0, Sr =1.0)

$\Pr$	Q	Du	C_f	Nu
0.71	1.0	0.2	2.4723	1.1434
1.00	1.0	0.2	2.4002	1.4343
0.71	2.0	0.2	2.4015	1.4422
0.71	1.0	0.6	2.5201	0.9809

Table 3 : Effect of Sc, K_r and Sr on C_f and Sh

(Gr =2.0, Gm =2.0, M =1.0, K =0.5, $\Pr$ =0.71, Q =1.0, Du =0. 2)

Sc	K_r	Sr	C_f	Sh
0.22	1.0	1.0	2.4723	0.9346
0.60	1.0	1.0	2.3332	1.4311
0.22	2.0	1.0	2.4424	1.0243
0.22	1.0	2.0	2.5125	0.8103

5 CONCLUSIONS

In this article a mathematical model has been presented for the Soret and Dufour effects on transient MHD flow past a semi-infinite vertical porous plate with chemical reaction. The non- dimensional governing equations are solved with the help of finite element method. The conclusions of the study are as follows:

1. The velocity increases with the increase thermal Grashof number and solutal Grashof number.

2. The velocity decreases with an increase in the magnetic parameter.

3. The velocity increases with an increase in the permeability of the porous medium parameter.

4. Increasing the Prandtl number substantially decreases the translational velocity and the temperature function.

5. Increasing the heat absorption parameter reduces both velocity and temperature.

6. The velocity as well as concentration decreases with an increase in the Dufour number.

7. The velocity as well as concentration decreases with an increase in the Schmidt number.

8. An increase in the Soret number leads to increase in the velocity and temperature.

9. The velocity as well as concentration decreases with an increase in the chemical reaction parameter.

References

Chamkha, A.J., Thkhar, H.S. and Soundalgekar, V.M. (2001): Radiation effects on free convection flow past a semi- infinite vertical plate with mass transfer. Chemical Engineering Journal. Vol.84, pp. 335-342. doi:10.1016/S1385-8947(00)00378-8

Eckert, E. R. G. and Drake, R. M. (1972): Analysis of Heat and Mass Transfer, McGraw-Hill, New York.

Helmy, K.A. (1998): MHD Unsteady free convection flow past a vertical porous plate. ZAAM, Vol.78, pp.255-270. doi:10.1002/(SICI)1521-4001(199804)78:4<255::AID-ZAMM255>3.0.CO;2-V

Ibrahim, F.S., Elaiw A. M. and Bakr, A. A. (2008): Effect of the chemical reaction and radiation absorption on the unsteady MHD free convection flow past a semi infinite vertical permeable moving plate with heat source and suction. Communications Nonlinear Science Numerical Simulation, Vol.13, pp.1056-1066. doi:10.1016/j.cnsns.2006.09.007

Jha, B. K. and Singh, A. K. (1990): Soret effects on free convection and mass transfer flow in the Stokes problem for an infinite vertical plate, Astrophys. Space Sci., Vol. 173, pp. 251 – 255 doi:10.1007/BF00643934.

Kafoussias, N. G., Nanousis, N. D. and Georgantopoulos, G. A. (1979): Free convection effects on the Stokes problem for an infinite vertical-limiting surface with constant suction, Astrophys. Space Sci.,Vol. 64a, pp. 391 – 399. doi:10.1007/BF00639516

Kafoussias, N. G. (1992): MHD thermal-diffusion effects on free-convective and mass transfer flow over an infinite vertical moving plate, Astrophys. Space Sci., Vol. 192, pp. 11 - 19. doi:10.1007/BF00653255

Kafoussias, N. G. and Williams, E. M. (1995): Thermal-diffusion and diffusion-thermo effects on mixed free-forced convective and mass transfer boundary layer flow with temperature dependent viscosity, Int. J. Engg. Sci., Vol.33, pp.1369 - 1384. doi:10.1016/0020-7225(94)00132-4

Lai, F.C. and Kulacki.F.A. (1991): Coupled heat and mass transfer by natural convection from vertical surfaces in a porous medium. Int. J. Heat Mass Transfer, Vol.34, pp. 1189-1194. doi:10.1016/0017-9310(91)90027-C

Nanousis, N., Georgantopoulos, G. and Papaioannou, A. (1980): Astrophys. Space Sci., Vol. 70, p.377. doi:10.1007/BF00639561

Soundalgekar, V. M. (1973): Free convection effects on the oscillayory flow past an infinite vertical porous plate with constant suction.Proc. Royal.Soc.London, Vol. 333, pp.25-36. doi:10.1098/rspa.1973.0045

Soundalgekar, V. M. (1977): Free convection effects on the Stokes problem for an infinite vertical plate, ASME, J. Heat Transfer, Vol. 99, pp. 499 – 501. doi:10.1115/1.3450729